Translated from *Uspekhi Khimii*, **57**, 832-855 (1988) U.D.C. 678.768:537.312

The Structure and Properties of Highly Conducting Polyacetylene Complexes

V.M.Skorobogatov and I.V.Krivoshei

The physicochemical characteristics of polyacetylene and its charge-transfer complexes have been examined. Data on the structural, electrical, magnetic, and optical properties have been discussed from a single viewpoint. Particular attention has been paid to a critical analysis of the soliton concept in relation to the structural and electrophysical properties. The probable mechanisms of the conductivity of polyacetylene have been examined.
The bibliography contains 118 references.

CONTENTS

I. Introduction 461
II. Electronic structure 462
III. Electrical properties 464
IV. Magnetic properties 466
V. Optical Properties 468
VI. Probable mechanisms of conductivity 469
VII. The structure of the conducting phase 471

I. INTRODUCTION

The first accurately solvable theoretical models used to study the electrical and magnetic properties of a solid were one-dimensional chains (for example the familiar models of Peierls, Ising, and Heisenberg). These one-dimensional models remained mathematical abstractions until the nineteen-seventies, when Shchegolev[1] drew attention to the possibility of obtaining real quasi-one-dimensional systems by chemical methods. This was soon followed by the description of the quasi-one-dimensional charge-transfer complex (CTC) TTF–TCNQ,† in which were detected not only metallic conductivity but also superconducting fluctuations close to 60 K. Although the latter were not confirmed, the sensational character of the report led to a rapid increase in the number of published papers on systems of small dimensions with unusual electrophysical properties.[2]

Polyconjugated organic polymers were the subject of detailed studies even in the nineteen-sixties, and important contributions to their study were made by Berlin, Cherkashin, Davydov, Liogon'kii, and others.[3,4] Almost all polyconjugated systems were found to be paramagnetics and semiconductors with interesting optical properties. Because of the low quality of the specimens, the impossibility of obtaining single crystals, and the uniformity of the principal characteristics, however, interest in the electrophysical properties of conjugated organic polymers decreased sharply in recent years. The renewal of interest in these materials is probably due to the discovery of the interesting properties of the inorganic polymer polythiazyl $(SN)_x$, whose single crystals show metallic conductivity under ordinary conditions, and become superconducting at T_c = 0.3 K.‡ Thus it has been shown that among polyconjugated compounds there are systems which do not contain a metal and which at the same time show metallic and even superconducting properties over a wide temperature range.

This striking result led to the discovery[5] of the unusual properties of the simplest polyconjugated organic polymer, polyacetylene $(CH)_n$, doped with electron donors or acceptors. As a result of doping, the specific conductance σ changes by many orders of magnitude, and, depending on the doping level, may take different values, typical of dielectrics, semiconductors, and even metals[6] (Fig.1).

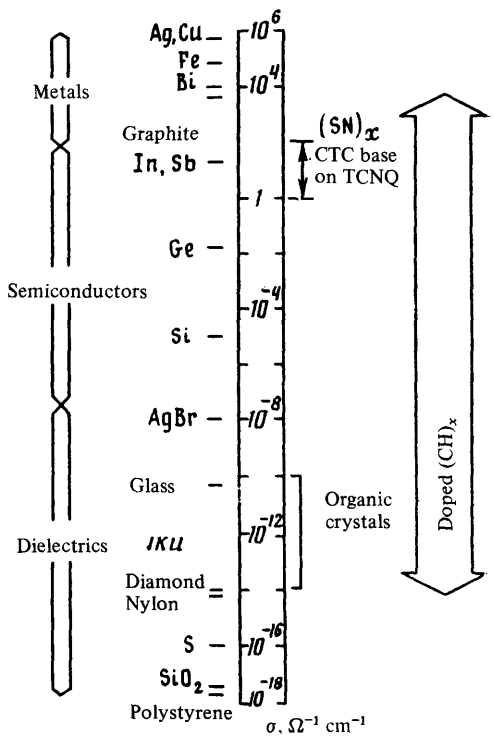


Figure 1. The specific conductance of doped PA and typical solids.[6]

† Here and subsequently, TTF = tetrathiafulvalene, and TCNQ = tetracyanoquinodimethane.

‡ See M.M.Labes, P.Love, and L.F.Nichols, Chem.Rev., 1979, 79, 1.

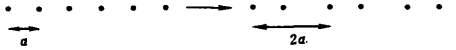
The simplicity of the molecular structure of polyacetylene (PA), the ease of obtaining high-quality films, and the possibility of varying their properties in planned fashion drew particular attention to PA. PA apparently provides an unprecedented example of a chemical compound whose properties have been studied using almost the entire range of physical methods. In theoretical chemistry and physics, PA provides a unique testing ground for that most modern (an popular) concept, the theory of solitons.

The main aim of the present review is to analyse the soliton concept, which is exotic in chemistry, but extremely popular in present-day physics. Since the soliton models of PA and analogous systems claim to provide a unique and systematic description and explanation of the principal physical properties, their examination is of considerable interest for the experimental and theoretial chemistry of conjugated polymers. The total number of published papers on PA is very large; it reached a maximum in 1983–1984, but had decreased considerably by 1987, while remaining high compared with other conducting polymers. Since PA is the prototype of all poly-conjugated organic systems, it is hoped that the present review will lead to a better understanding of other polymers such as poly-*p*-phenylene, polypyrrole, polythiophen, etc.

II. ELECTRONIC STRUCTURE

For many years the efforts of chemists have been concentrated on the synthesis of polyconjugated compounds with the longest possible chain. These studies have been based on both simple quantum-chemical calculations by the Hückel method and experimental data on the optical and electrical properties of model low-molecular-weight systems, according to which the width of the energy gap E_g (that is the energy of the transfer of a π-electron from the ground state to the lowest excited singlet state) and hence σ increase with increase in the number of conjugated units N_{C-C}. In the limiting case as $N_{C-C} \to \infty$, the electrons should be completely delocalised, the bonds beween the C atoms should be completely equivalent, and the ground state of the polymer should become metallic. Among the vast number of compounds synthesised, however, it has not been possible to discover one whose electrophysical properties are not semiconducting. This has led to a number of phenomenological explanations, details of which can be found in familiar monogaphs.[3,4] A significant feature is that all the explanations have taken into account not the intrinsic electronic properties of the polyene chain but numerous secondary factors, chiefly conjugation defects and disorder in the supermolecular structure.

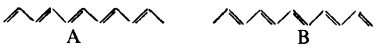
This situation apparently arose because of the sharp separation between the chemistry of macromolecular compounds and solid-state physics. At the same time, for physicists, this problem had been settled long before: the impossibility of the metallic state in one-dimensional systems follows from Peierls' theorem, according to which a regular one-dimensional chain of atoms is unstable with respect to deformation leading to doubling of the lattice period *a*:



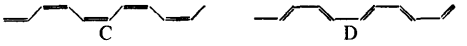
The change from a structure with equalised bonds to a structure with alternation of the bonds is called a Peierls transformation. In the band theory of solids, in the Peierls phase, the conductivity band is split exactly in the middle, as a result of which this phase is dielectric. The Peierls transformation is energetically favourable as a result of the lowering of the total energy of the lattice. This instability is characteristic of any one-dimensional metal, and the nature of the distortions is determined by the degree of filling of the conductivity band: if $1/n$ is the degree of filling of the band, then the change to the dielectric state is associated with *n*-merisation of the lattice. Since for PA, $n = 2$, there should be alternation of the double and single bonds in the chain. The alternation of the bonds in PA can now be regarded as a factor established experimentally from X-ray[7] and electron[8] diffraction data and from solid-state NMR spectra;[9,10] the difference between the lengths of the double and single bonds is 0.06–0.08 Å.

Thus an ideal crystal of PA should be a dielectric. At the same time, the experimental values of σ show a wide scatter, $10^{-5}-10^{-12}$ Ω^{-1} cm^{-1}.[11,12] The comparatively high values of σ are due to defects of different kinds in the molecular and crystal structure of real specimens; the paramagnetic defects are of particular interest. Polyacetylene exists as *cis*- and *trans*-isomers; the former is thermodynamically stable only at low temperatures, and is the main product of the catalytic polymerisation of acetylene by the most widely used method of Shirakawa.[13] The paramagnetism of PA is due entirely to the presence of the *trans*-isomer, and on thermal isomerisation (which is irreversible, because of side reactions leading to cross-linking of the chain and partial degradation of the polymer), the increase in the proportion of the *trans*-segments is accompanied by an increase in the concentration of spins and an increase in σ.[12]

For the subsequent discussion it is important to note that the ground state of *trans*-PA is doubly degenerate: change in the alternation sequence does not alter the energy. Thus the existence of two resonance phases A and B of equal energy is possible:



There is no degeneracy in *cis*-PA: change in the alternation sequence converts the *cis*-transoid phase C into the less stable *trans*-cisoid phase D:



It was the energetic equivalence of the phases A and B that provided the basis of the solution model of *trans*-PA, better known as the Su–Schrieffer–Heeger (SSH) model.[14] Strictly speaking, a soliton is an isolated wave, which retains its structure after collision with any other isolated wave of the same type. In solid-state physics, the term solitons is usually employed to describe non-linear excitations leading from one potential energy minimum to another with the same energy, and they are regarded as quasi-particles. In the case of *trans*-PA, a soliton is a topological defect in the alternation, extending over several bonds, so that the phase A is gradually converted into the phase B:



In the SSH model, the *trans*-PA chain is represented by a one-dimensional lattice with an elastic constant *K*, at each site of which there is one π-electron and phonon interactions are taken into account by a Hamiltonian of the form:[14]

$$H = \sum_{n,S}^{N} \beta_{n,n+1} (a^{+}_{n,S} a_{n+1,S} + a^{+}_{n+1,S} a_{n,S}) + \frac{1}{2} K \sum_{n} (u_n - u_{n+1})^2$$

The first summation is the Hückel Hamiltonian for N electrons, written in the representations of secondary quantisation, where $\beta_{n,n+1}$ is the resonance integral of the bond between the atoms with numbers n and $n + 1$, and $a^{+}_{n,S}$ *and* $a_{n,S}$ the operators of the generation and annihilation of π-electrons in the states with number n and spin S. The second summation represents the energy of the elastic lattice with displacements u_n of the lattice sites from their equilibrium positions. Thus $\beta_{n,n+1} = \beta_0 - \alpha(u_{n+1} - u_n)$, where α is the electron–phonon interaction constant. If only the electronic energy is taken into account, the one-dimensional lattice will be unstable with respect to Peierls doubling of the lattice period, and will be

transformed into the state with alternation of the bonds. Doubling corresponds to the condition $u_n = (-1)^n u_0$, where u_0 is the displacement of the lattice sites in the defect-free chain of *trans*-PA. Thus a gap $E_g = 2\Delta = 8\alpha u_0$ is produced between the valence band and the conductivity band. The soliton excitations are introduced by means of the function

$$\Delta_n = \Delta \text{th}(na/l) \quad (1)$$

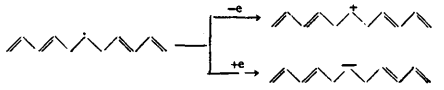
where l is the half-width of the soliton, whose wavefunction has the form

$$\Phi_n = l^{-1/2} \cos(\pi n/2) \text{ sech } (na/l) \quad (2)$$

Thus in the SSH model, solitons appear not from the internal structure of the solution, but as localised electronic states in the centre of the gap with the given topology of the defect. In view of the considerable computational difficulties, the SSH Hamiltonian allows only a numerical solution. When the parameters E_g + 1.4 eV, band width $4\beta_0$ = 10 eV, and K = 21 eV Å^{-2} are used, the SSH model gives the energy of the soliton $E_s = 2\Delta/\pi \simeq 0.42$ eV and $l = 2\beta_0 a/\Delta = 7a$. The relatively large size of the soliton compared with the lattice period shows that the discrete character of the lattice plays practically no part, and that the energy of the capture of a soliton by a lattice site does not exceed several meV. The effective mass of the soliton is only a few times greater than the mass of the electron, so that the soliton has a very high mobility.

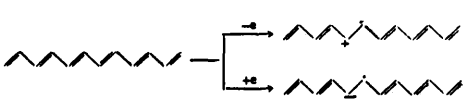
In the continuum model[15] [$na = x$; $\Delta_n \rightarrow \Delta(x)$], the function (1) strictly describes the configuration of the ground state with the boundary conditions $\Delta(x) \rightarrow \pm\Delta$ as $x \rightarrow \pm\infty$. Unlike the discrete SSH model, the continuum model makes it possible to obtain analytical solutions. In most cases the results of calculations using the two models agree qualitatively, although the concrete definition of the structure of the soliton in the discrete model makes it possible to take account of various fine effects.

The solitons just examined have spin, but not charge, so that they are responsible for the paramagnetism of PA, but are not current carriers. The role of carriers is played by spin-free charged solitons, which should be produced by the reaction of a donor or acceptor of electrons with defect chains of *trans*- PA:

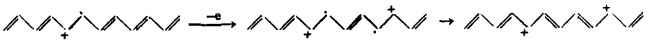


From a chemical viewpoint, neutral solitons S$^{\cdot}$ are radicals, positive solitons S$^+$ are carbocations, and negative solitons S$^-$ are carbanions, and in all cases the electron density is delocalised over a certain section of the chain with length $2l$. Fig.2 illustrates the situation in the representations of the band structure of solids.

Thus PA becomes a conductor as a result of doping and the associated rearrangement of the electronic structure, and not as a result of a phase transformation of the chain into a metastable state, which is not produced in compounds of this class. In other words, the electron or hole formed as a result of doping and charge transfer, after a certain characteristic time, are converted into a localised state with the formation of a soliton. If the doping reaction involves not only defect chains having spin but also defect-free chains, then solitons should be generated in pairs.[14] Numerical calculation[16] shows that with slight doping, the energetically preferred formation is not a non-bonded soliton–soliton pair S$^{\pm}$–S$^{\cdot}$ but a polaron P$^{+\cdot}$ (in other words a radical-ion), representing a bound state:



The phases of the alternation on the two sides of the soliton are opposed, whereas the formation of a polaron does not lead to changes in the phases. Two symmetry levels now appear in the energy gap (Fig.2), one of which is situated ~0.3 eV above the top of the valence band, while the other is situated at the same distance below the bottom of the conductivity band. On further doping, two processes compete with one another; the polaron states begin to form a band, and neighbouring polarons may recombine to give spin-free bipolarons (carbodications):



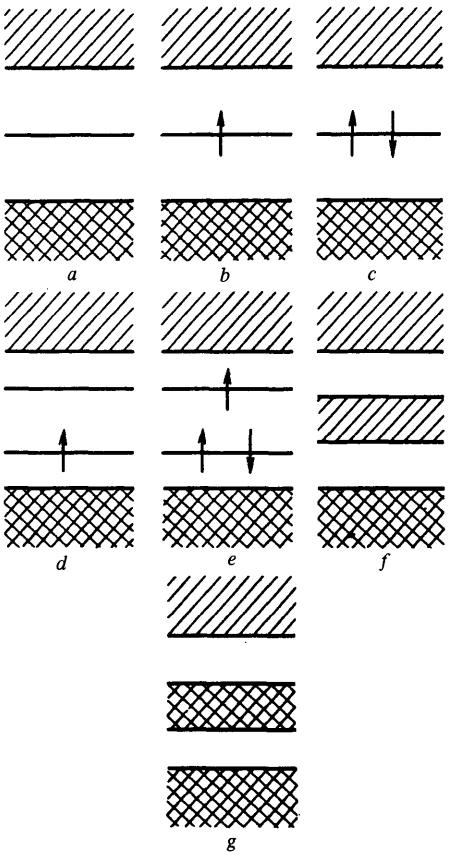


Figure 2. The band structure of states of the soliton type with charge q and spin S: *a*) positive soliton S$^+$ ($q = +e$, $S = 0$); *b*) neutral soliton S$^{\cdot}$ ($q = 0$, $S = 1/2$; *c*) negative soliton S$^-$ ($q = -e$ $S = 0$); *d*) positive polaron P$^+$ ($q = +e$, $S = 1/2$); *e*) negative polaron P$^-$ ($q = -e$, $S = 1/2$); *f*) soliton lattice S$^+$ ($q = Nye$, $S = 0$); *g*) soliton lattice S$^-$ ($q + -Nye$, $S = 0$).

Because of the degeneracy of the ground state of *trans*-PA, the bipolarons are unstable, and dissociate to give charged solitons forming a conductivity band within the gap (Fig.2). The conductivity is now due not to jumps between localised soliton states but to the soliton band. This band subsequently becomes broader, and finally joins up with the top of the conductivity band and the bottom of the valence band, the gap collapses, and the highly doped PA becomes a quasi-metal with ordinary electronic conductivity.

Thus for highly conducting complexes of PA, two fundamentally different conductivity mechanisms are postulated. The first is due to the movement of quasi-particles—spin-free charged solitons (or bipolarons)—which are combined with distortions of the lattice and which form a band (either completely filled or unpopulated) within the gap. The novel and unique character is revealed in highly doped specimens and is associated with the ordinary movement of electrons as a result of the overlap of the conductivity, valence, and soliton bands.

The polaron model is more general than the soliton model, since it does not require degeneracy of the ground state. This requirement, generally speaking, is extremely strict, and is not satisfied even for *cis*-PA. Nevertheless, the electrophysical properties of the two isomers are completely analogous; moreover, analogous properties are shown by poly-*p*-phenylene, polypyrrole, and other polymers, for which there is no degeneracy. Between the soliton and polaron models of PA, however, there is a deep internal relationship, which follows from relativistic φ^4 field theory;[17] a universal method for obtaining soliton, polaron, and other quasi-particle solutions has been proposed, for example, in Ref.18. The large number of modifications of the SSH model will not be discussed (the interested reader can find details in a published review[19] and the references therein), and attention will be concentrated on the cardinal question of whether the soliton theory is in fact necessary and sufficient to explain the properties of PA and, in the wider sense, all conducting polymers.

III. ELECTRICAL PROPERTIES

The general character of the changes in the static electrical conductivity σ when PA is doped with various typical acceptors to the maximum levels attainable experimentally is shown in Fig.3,[20] where y denotes the number of moles of dopant per mole of CH units. Thorough studies[21] showed that the detailed form of the $\sigma(y)$ relationship is determined by the previous history of the specimens: the method used to synthesise the PA, the isomeric composition, the type of dopant, and, to the greatest extent, by the method of doping. In general, it is assumed[21] that the slower the introduction of the dopant, the narrower the range of values of y within which the main increase in the electrical conductivity takes place. For example, when *trans*-PA is doped with iodine vapour at $p \leqslant 0.1$ mmHg, σ increases by a factor of 10^4 in the range $10^{-3} \leqslant y \leqslant 10^{-2}$.[21] On the other hand, the $\lg\sigma - \lg y$ graphs obtained by doping *cis*- and *trans*-PA with AsF_5 vapour at different pressures[21] were practically linear throughout the range of values of y, and the same results were obtained when PA was doped rapidly (p = 0.3 mmHg) with iodine vapour.[22] The dependence of the thermo-EMF on the doping level is also determined by the rate of doping;[21,23] the lower the rate of doping of PA, the narrower the range of values of y within which the thermo-EMF decreases from the values typical of semiconductors ($\sim 10^3$ μV K^{-1}) to the values typical of metals (~ 10 μV K^{-1}).

The observed effects are usually attributed to the more or less uniform distribution of the dopant throughout the volume of the PA specimens. It is assumed that the most uniform distribution is achieved with so-called cyclic doping. In this method, the exposure of the film of PA to the vapour of the dopant, for example AsF_5 (at T = 143 K, $p < 0.1$ mmHg), is alternated either with evacuation or with freezing-out the non-absorbed AsF_5 at 7 K,[21,23,24] and this procedure is repeated until the required doping level is achieved. Thus the experimental justification for the theory of uniform doping is the exceptional sensitivity of various electrophysical characteristics to the doping method: the more uniform the distribution of the dopant, the sharper the semiconductor–metal transition.

At the same time, it follows from even simple estimates of the entropy effects and the energy of lattice deformation on doping[25] that aggregation of the dopant in stacks or layers is energetically preferable to its random distribution (with the possible exception of the small Li^+ ions). Direct measurements of the distribution profiles by electron-probe X-ray microanalysis[26] in all cases showed an extremely non-uniform distribution of the dopants at low values of y even in thin PA films (~ 10 μm), and relatively uniform distribution was achieved only by doping to y_{max}. The effect achieved by cyclic doping is not clear; it is not fully understood how repeating the low-temperature cycles is able to achieve the required uniformity.

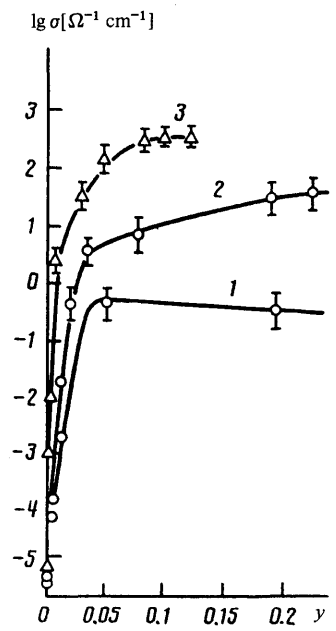


Figure 3. Dependence of the electrical conductivity of PA on the doping level;[20] *1*) $(CHBr_y)_x$, *2*) $(CHI_y)_x$, *3*) $[CH(AsF_5)_y]_x$.

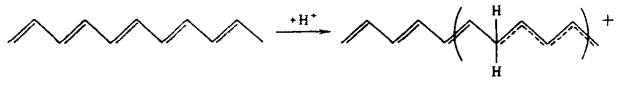
Thus diffusion is an activated process, and its rate decreases exponentially with temperature. It is significant that the characteristic distribution profiles of the dopant into the bulk of the specimens remain completely unchanged even when the films are kept for one week in a dynamic vacuum.[27] This phenomenon is probably due to fixation of the dopant as a result of chemical reactions, so that free diffusion stops. For the same reason, deviation from Fick's law is observed, as shown in experiments[28] on the kinetics of diffusion.

Unfortunately, there are extremely few published data on the chemistry of the reactions of PA with dopants. Extensive photoelectron, Mössbauer, and Raman spectroscopic data make it possible to formulate the most extensively studied reactions as follows:

$$2(CH)_x + 3y\,AsF_5 \rightarrow 2[(CH)_x^{y+}(AsF_6^-)_y] + y\,AsF_3$$
$$(CH)_x + 2y\,FeCl_3 \rightarrow [(CH)_x^{y+}(FeCl_4^-)_y] + y\,FeCl_2$$
$$2(CH)_x + 3y\,I_2 \rightarrow 2[(CH)_x^{y+}(I_3^-)_y]$$

The actual situation, however, is much more complex than indicated by these simple equations. After doping with AsF_5, the composition of the specimens usually corresponds to the formula

$[CH(AsF_n)_y]_x$, where $5 \leqslant n \leqslant 6$,[29] depending on the doping conditions. In addition to I_2 molecules, $(CHI_y)_x$ contains the ions I_5^-, I_3^-, and I^-,[30] and when bromine is used as dopant, most of it adds on across the double bonds of PA, forming saturated segments $-CHBr-CHBr-$.[31] Some dopants undoubtedly form covalent bonds with PA, as shown for bis(fluorosulphuryl)peroxyl [32] and trimethyloxonium salts, which are effective CH_3^+ cation donors.[33] Doping by protic acids which are not oxidising agents, for example, HF, apparently takes place by the same mechanism:[34]



In published discussions of the $\sigma(y)$ relationships, however, the independent variable y taken is always the total analytical concentration of the dopant, which is found either gravimetrically or (for the smallest values of y) using tracer atoms. It is assumed *a priori* that all the absorbed dopant forms a highly conducting complex with PA. This assumption is in general incorrect; spectrophotometric analysis of the equilibria by the Benesi–Hildebrand method in $PA-I_2$ [35] and $PA-Br_2$ [36] systems showed that the composition of the conducting complexes corresponds to the formula $[(CN)_n(X_2)]$, where X = I or Br, and $(CH)_n$ is a segment of the continuous conjugation ($n < x$). Thus S_3^- ions may also be produced by side reactions which are not related to the formation of conducting complexes. Additional evidence in support of this conclusion is apparently provided by data on the thermal desorption of iodine from $(CHI_7)_x$:[37] treatment of the specimens at 383 K for 105 min lowered the conductivity by a factor of 10^4 with a decrease in y by a factor of 5, but at the same time the intensity of the band at 107 cm^{-1} in the Raman spectrum due to I_3^- ions increased by a factor of 14.

The formation constants of $[(CH)_n(I_2)]$ and $[(CH)_n(Br_2)]$ are 64 $mole^{-1}$ and 8 $mole^{-1}$ respectively, and the concentrations of the active states in PA accessible for complex formation at 0.4 mole dm^{-3} for I_2 and 0.9 mole dm^{-3} for Br_2.[35,36] Thus many of the properties of doped PA are determined by the chemical character of the dopant. Thus it has been shown[35] that for the overall formula $(CHI_{0.25})_x$, the equilibrium composition which is entirely responsible for the electrical conductivity corresponds to the formula $(CHI_{0.008})_x$.

Thus for the vast majority of dopants, the true concentration dependence $\sigma(y)$ must be regarded as unknown. The same is true of the concentration dependence of the thermo-EMF. For its determination, it is necessary to take as independent variables not the total but the equilibrium concentrations of the dopants. Thus use of the equilibrium concentrations may lead to radical changes in the established relationships between the composition and properties of PA. From the classical relationship for semiconductors

$$\sigma = c\mu e \qquad (3)$$

where c is the concentration of the carriers, μ their mobility, and e the charge of the electron, it follows that σ is linearly dependent on the equilibrium concentration of the conducting complex. In fact, the dependence is exponential,[35,36] as is characteristic of the Mott mechanism of conductivity in disordered solids, which involves jumps of variable length between localised states.[38] Data obtained at room temperature[35,36] show very good agreement (correlation coefficient 0.995) with the Mott law $\sigma \sim \exp(-T^{-1/4})$ throughout the range studied, $0.007 \leqslant y \leqslant 0.25$. Thus the use of the equilibrium concentrations shows that there are no signs of a semiconductor– metal transformation and hence of a change in the mechanism of the conductivity, at least in this range of nominal values of y.

Representation of the data[35,36] in the form of the usual $\sigma(y)$ relationships gives typical *S*-shaped curves. On these graphs it is possible to distinguish three regions. In the first ($y \lesssim 10^{-4}-10^{-3}$), the $\sigma(y)$ dependence is weak; in the second ($10^{-3} \lesssim y \lesssim 10^{-2}$), the $\sigma(y)$ dependence is very strong, and this is interpreted as a semiconductor–metal transformation;[21,39] in the third, quasi-metallic, region, the conductivity is saturated (the values of y_{max} depend on the nature of the dopant). According to the soliton model, the change from one region to another should be accompanied by a change in the conductivity mechanism. The chief test for identifying the mechanisms is the temperature dependence of σ. Considerable efforts have been made to establish the $\sigma(T)$ relationships as accurately as possible, but in spite of the large amount of experimental data, no clear and systematic picture has yet been revealed. Typical graphs[39,40] are shown in Fig.4, and lead to two conclusions. Firstly, in all cases the temperature dependence is activational, but with increase in y the $\sigma(T)$ dependence becomes weaker (for dopants such as AsF_5,[39] $FeCl_3$,[41] and $(FSO_2O)_2$ [32] in the range 300–250 K, even a slight increase in σ, corresponding to the behaviour of metals, is observed). Secondly, there is no clearly defined phase transformation, which would have been revealed by an abrupt change in the $\sigma(T)$ relationship at a certain critical concentration of the dopant.

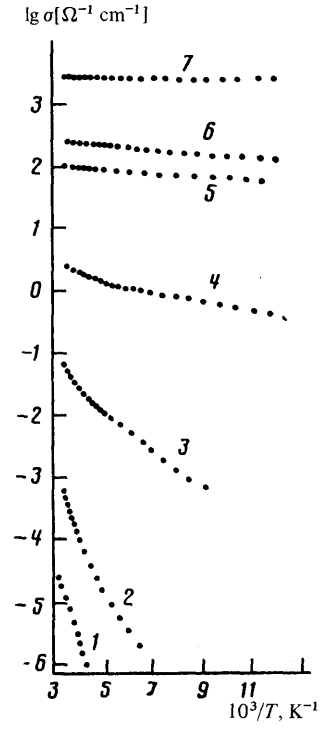


Figure 4. Temperature dependence of the electrical conductivity of $[CH(AsF_5)_y]_x$ [39] for y = 0 (*1*), 0.0028 (*2*), 0.0059 (*3*), 0.010 (*4*), 0.050 (*5*), 0.10 (*6*), and 0.14 (*7*).

For the analytical description of the $\sigma(T)$ dependence, different authors have used relationships of the form $\exp(-T^{-1})$, $\exp(-T^{-1/4})$, $\exp(-T^{-1/2})$, or T^x, where $x > 10$ (see the literature cited in Ref.11). This variety suggests that in fact, none of the proposed relationships is satisfied over a sufficiently wide range of temperatures. The same conclusion was reached after detailed $\sigma(T)$ measurements for $(CHI_y)_x$ specimens with different previous histories;[11] any functional relationship provided a satisfactory description of the experimental

data only in a more or less limited temperature range. It should be emphasised that, unlike the $\sigma(y)$ relationships, the $\sigma(T)$ relationships were found to be independent of the method used to dope PA.[42] If however the published conclusions[21,23] regarding the fundamental influence of non-uniform distribution of the dopant on the electrical properties of PA are accepted, then it is impossible to explain why these non-uniformities (or their absence) have no influence on the nature of the fundamentally more important $\sigma(T)$ relationships.

Generally speaking, the lack of agreement and often the direct contradiction between different experimental data on the electrical properties of PA are to a large extent due to the extremely complex morphology of the specimens, which makes correct measurements extremely difficult. In most photomicrographs obtained using the scanning electron microscope, PA films and powders appear as accumulations of disordered intertwined fibrils with a thickness of 10–80 nm and a length of tens of nm.[13,20] In films obtained by the standard method of Shirakawa, the volume fraction of the fibrils is ~40%. These fibrils in turn are made up of disordered, twisted, and intertwined micro-fibrils with a thickness of 3–5 nm.[43] On the other hand, transmission photographs show the presence of lamellae with a diameter of several tens of nm and a thickness of several nm; these lamellae combine in irregular stacks to form pseudo-fibrils.[6] High-resolution electron microscope data[44] show, however, that the morphological sub-units of both the original and the doped PA are globules with a diameter of 20–50 nm. These globules combine to form clusters, monolayers, or fibril-like formations, that is secondary structural elements. These elements then form tertiary structures: lamellae (monolayers lying on top of one another), loose networks, and their combinations with relative contributions determined entirely by the synthesis conditions. In freshly prepared PA, the globules are apparently joined to one another only by cohesive forces. Thus the polymerisation of acetylene in the presence of surface-active substances gives emulsions with spherical PA particles;[45] ultrasonic dispersal of the PA suspensions gives colloidal solutions.[46]

In one way or another, the basic structure of PA may become similar to a highly porous sponge with a specific surface of 35–60 $m^2\ g^{-1}$.[20,47] The electrical resistance of these specimens is made up of many terms which depend on temperature in different ways: the resistance of the inter-crystallite contacts within each fibril or globule, the resistance of the inter-fibril or inter-globule contacts, the resistance of the amorphous phase, and also terms determined by the high anisotropy of the three principal components of the specific conductance tensor. The macroscopic conductivity should naturally be determined by the largest of these resistance terms, but the real picture is complicated considerably when account is taken of geometric factors (the maximum specific resistance does not always correspond to the maximum resistance) and the fact that the ratio of the different components of the resistance may change with change in temperature. As a result, the $\sigma(T)$ relationship for non-crystalline specimens generally does not reflect the properties of the conducting complexes, and the data leave wide scope for speculation.

At the same time, unambiguous information on the intrinsic $\sigma(T)$ relationship can be obtained by the simple and elegant method of short-circuited potential electrodes (SPE), which eliminates the influence of the resistance of the inter-crystallite contacts and the small components of the specific conductance tensor.[48] The SPE method is qualitative, but it makes it possible to deduce the true temperature dependence of the largest of the components of the specific conductance tensor, by predicting the general course of the relationship for single crystals. The data obtained[49] by the SPE method at $T \geqslant 77$ K for highly conducting PA specimens (Fig.5) show that the true $\sigma(T)$ relationship has the form typical of metals, and is independent of the morphology of the PA. For $[CH(FeCl_3)_{0.06}]_x$, the SPE method established metallic behaviour as far as $T = 1.9$ K.[50]

IV. MAGNETIC PROPERTIES

The magnetic properties of PA have attracted particular attention from the very beginning. The experiments have been designed to answer the questions, of fundamental importance for the soliton concept, of whether the unpaired electrons are in fact highly mobile, whether their diffusion is chiefly one-dimensional, and whether at medium doping levels the paramagnetism disappears and the charge is carried by spin-free solitons.

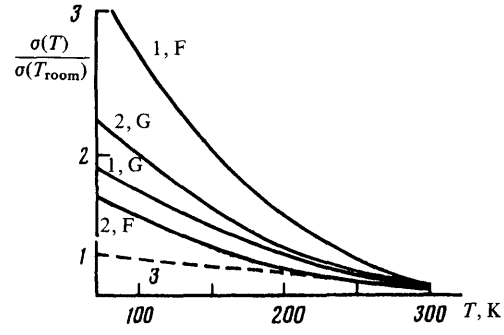


Figure 5. Temperature dependence of the reduced electrical conductivity, obtained by the SPE method;[49] *1*) $[CH(ClSO_3H)_y]_x$, *2*) $[CH(NOClO_4)_y]_x$ (*G* = globular PA, F = fibrillar PA); *3*) current-carrying silver paste.

An important factor for a theoretical description is how the spin density is distributed along the PA chain. The first source from which attempts were made to extract this information was EPR data.[51,52] The spectrum of PA contains an intense singlet with a width of several G, whose characteristics depend markedly on the previous history of the specimen.[12] The paramagnetic of PA is not associated with the charge carriers; treatment with ammonia lowers the conductivity by several orders of magnitude, but does not alter the EPR spectrum.[52] The experimental form of the EPR line is effectively reproduced[51] if the SSH spin wavefunction in form (2) is adopted. These and other similar calculations (see for example Refs. 53 and 54), however, do not take account of all the parameters determining the EPR spectra of π-electron radicals: the anisotropy of the *g*-value and the hyperfine interactions (HFI), the relative orientation of the tensor elements, and relaxation processes. Definite conclusions about the HFI and the number of nuclei involved in the interaction with the soliton can hardly be reached by modelling a singlet EPR line with an unresolved hyperfine structure (HFS). It has been correctly pointed out[55] that from the mathematical viewpoint, this is equivalent to solving one equation with many unknowns. As a result, a large number of wavefunctions, completely dissimilar to the function (2), are capable of reproducing the experimental EPR spectra equally successfully.

More reliable information on the distribution of spin density can be obtained by double electron–nuclear and triple electron–electron–nuclear resonance (ENDOR and EENTOR respectively): the ENDOR spectra are characterised by two and only two individual sets of HFI tensors for the C and H nuclei, and in the EENTOR spectra the relative intensities of the signals reflect directly the proportions of the nuclei involved in a given HFI.[56] It follows from ENDOR that in *trans*-PA, neighbouring C atoms are magnetically non-equivalent, and the spin densities on them are $\rho_1 = |0.06|$ and

$\rho_2 = |0.02|$, and from EENTOR it follows that they have opposite signs: $\rho_1 = +0.06$, $\rho_2 = -0.02$. Thus the unpaired electron must be delocalised over approximately 50 C atoms. This estimate seems too high. The accuracy of the determination of the absolute values of ρ, which depends on the choice of model used to calculate the components of the tensors, should not be overestimated; other data[57] indicate the value $\rho \geqslant 0.01$. The ratio $\rho_2/\rho_1 = -0.33$, found directly from the ENDOR line, is more correct.[58] Since negative values of ρ can appear only as a result of Coulombic interactions (the potential of the single-site electron–electron repulsion, estimated by the Hartree–Fock method, is ~ 3 eV [58]), it is clearly necessary to take account of electron correlations. The neglect of these correlations is probably the most significant unsatisfactory feature of the SSH model.

The main evidence of the unique character of the spins in *trans*-PA is the difference in the behaviour of the PA isomers, established in experiments[53] on the dynamic polarisation of the nuclei (DPN). These experiments involve the measurement of the dependence of the amplitude of the ^{1}H NMR signal at the nuclear Larmor frequency ω_n on the frequency of the microwave pumping, close to the electronic Larmor frequency ω_e. For mobile spins, the signal is amplified on pumping at a frequency ω_e (the so-called Overhauser effect). If however the spins are fixed (the frequency of their jumps is lower than ω_n), then the signal is amplified on pumping at a frequency $\omega_e + \omega_n$ and is weakened in the case of the frequency $\omega_e - \omega_n$ (the so-called solid-state effect). In fact, at room temperature, the Overhauser effect was observed in *trans*-PA, and the solid-state effect in *cis*-PA. Quantitative estimates of the dynamics of the spins and the dimensions of their diffusion[53] were obtained from the frequency dependence of the proton spin–lattice relaxation time T_{1H}. If the diffusion is one-dimensional, and the protons relax on the diffusing spins, then the relationship $f(\omega) = (2D_{||}\omega)^{-1/2}$ is fulfilled, where $f(\omega)$ is function of the spectral density, and $D_{||}$ the diffusion coefficient of the spins, related to the coefficient of translational diffusion by the relationship $D'_{||} = a^2 D_{||}$. From the experiments[53] it follows that $D_{||} = (3-6) \times 10^{13}$ s^{-1}, and the anisotropy of the spin diffusion is $D_{||}/D_{\perp} \simeq 10^6$.

The $T_{1H}^{-1} \sim \omega^{-1/2}$ relationship is not specific for one-dimensional diffusion, however, and may also be determined by nuclear spin diffusion (NSD) to fixed electronic spins, taking place by a reorientation of the nuclear spins with their subsequent relaxation on paramagnetic centres. Measurements of T_{1e} by the spin-echo method[59] show that the NSD model describes the experimental data no less satisfactorily than the one-dimensional model,[53] although the anisotropy and delocalisation of the solitons are completely neglected. The adequacy of the NSD model is confirmed by a large amount of ^{1}H, ^{2}H, and ^{12}C NMR data (see for examples Refs.60–62), and from spin-echo measurements[63,64] it follows that there are several types of paramagnetic defect. The high-resolution DPN spectra[10] reveal a solid-state defect in *trans*-PA even at room temperature. The great majority of continuous conjugation segments in *trans*-PA obviously do not contain highly mobile spins; otherwise, the movement of the solitons along the chains would have led to dynamic averaging of the bond lengths, that is to the suppression of alternation, and this does not agree with experiment. Although the discussion of the paramagnetic defects in PA is not complete, it may be concluded that the various magnetic resonance methods up to the present have provided information on those properties of the topological defects which are determined by their local structure, and not on their kinematic properties.

In non-doped PA, the paramagnetism obeys the Curie law. It would seem that proof of the inverse relationship between the charge and spin of the current carriers, predicted by the soliton model, should be easily obtained by measuring the dependence of the magnetic susceptibility on the doping level. Up to the present, however, irrefutable data have not been obtained. Measurements made by the Faraday method[65] and the Schumacher–Slichter method, based on a combination of NMR and EPR,[24] show a regular decrease in the temperature-independent Curie susceptibility χ_C and the absence of temperature-independent Pauli susceptibility χ_P when *trans*-PA is doped with moderate amounts of AsF_5. On the other hand, according to EPR data,[66] doping *cis*-PA leads to the rapid appearance of χ_P and its regular increase in proportion to y. A comparative EPR study[67] of the doping of *cis*- and *trans*-PA with AsF_5 only partly resolved the contradictions, by confirming that doping *cis*-PA is accompanied by an increase in χ_P, whereas in cyclically doped *trans*-PA, χ_P is negligibly small. These phenomena were again attributed to the non-uniform doping of *cis*-PA.

The quantitative determination of the concentration of spins [S$^\cdot$] in highly conducting materials encounters fundamental difficulties; increase in σ is accompanied by a greater skin-effect, produced when the thickness of the skin-layer and the characteristic dimensions of the specimen are comparable. The EPR line becomes asymmetrical, and no longer gives quantitative information on [S$^\cdot$]. Faraday's method,[65] which does not have this disadvantage, measures the total static magnetic susceptibility $\chi = \chi_D + \chi_C + \chi_P$, where χ_D is the diamagnetic component, which must be calculated from the Pascal constants. The accuracy of these calculations is undoubtedly low, because of the lack of accurate information on the state of the dopant in PA and the uncontrolled defects in the molecular structure of PA. Moreover, it is necessary to calculate the difference $\chi - \chi_D$; these quantities are of the same order of magnitude, and are greater than χ_C and χ_P by 1–2 orders of magnitude, so that the subtraction unavoidably leads to a high loss of accuracy.

The adequacy of the Schumacher–Slichter method[24] has not been established. For example, measurements of χ for $(CHBr_y)_x$ specimens by the Faraday method give $\chi_P \simeq 0$ for $0 < y < 0.02$, and $\chi_P \geqslant 4 \times 10^{-6}$ CGS units per mole of C for $y > 0.02$, whereas according to the Schumacher–Slichter method, $\chi_P \lesssim 10^{-8}$ CGS units per mole of C, irrespective of y.[68] The most convincing data are apparently EPR data[69] obtained for $[CH(AsF_5)_y]_x$ specimens prepared as extremely thin needles, which prevented complications resulting from the skin-effect. Irrespective of the isomeric composition of PA, at $T \lesssim 50$ K, superposition of two EPR lines with the same g-value, one narrow and one broad, was observed. The characteristics of the narrow line make it possible to assign it to conductivity electrons, responsible for χ_P. A remarkable feature is that χ_P increases regularly with increase in y in the same sense as the elecrical conductivity, from which it clearly follows that the current carriers in $[CH(AsF_5)_y]_x$ are classical in character. At the same time, the broad line is associated with localised electrons, responsible for χ_C; after the specimens have been treated with ammonia, only the broad line remains in the spectra. The same behaviour is characteristic of $[CH(SbF_5)_y]_x$.[69]

When PA is doped with iodine, the picture changes. EPR data[21,7] show a gradual decrease in the intensity of the signal and its complete disappearance in highly doped specimens, but the Faraday method[71] detects quite significant Pauli paramagnetism ($\chi_P \leqslant 2 \times 10^-$ CGS units per mole C). Other Faraday measurements,[72] however, do not show any significant χ_P, and the same result was obtained b EPR.[73] In Ref.73, however, in contrast to Refs.21 and 70, it was noted that with increase in the doping level, after the initial sharp decrease, the value of χ_C at $y \geqslant 0.1$ becomes constant. A more systematic picture was obtained when the EPR measurements were extended into the range of helium temperatures.[74] It was found tha not only the spin susceptibility, but also [S$^\cdot$], depend on temperatur and at $T \leqslant 10$ K, the values of [S$^\cdot$] are almost the same for the doped and non-doped specimens. Thus the absence of the EPR signal at high temperatures is directly related to the high conductivity; at y_{max}, the signal is not detected even at $T = 4.2$ K.

The characteristic features of the EPR in $(CHI_y)_x$, and also in $(CHBr_y)_x$, can be explained using the ideas developed for disordered semiconductors,[38,75] in which the EPR signal is usually due to defects in the crystal structure. This signal often disappears when the semiconductor is doped. On the other hand, an EPR signal due to lattice defects is not observed in any metal. This may be due either to the shielding by the conductivity electrons of the Coulombic repulsion between defect states having spins or to the hybridisation of the wavefunctions of localised electrons and conductivity electrons. Similarly, the magnetic properties of $(CHI_y)_x$ may be due to the interactions of localised and band states. Doping generates Pauli spins, which do not give an EPR signal, because of strong spin–orbit scattering on iodine, but which interact with Curie spins. As a result, the paramagnetism is determined both by Coulombic interactions between the localised states and by hybridisation of localised and band states; the increase in the hybridisation with increase in y may lead to the apparent disappearance of the local magnetic moment. In highly doped $(CHI_y)_x$, even at helium temperatures the conductivity is high, and no EPR signal is observed. This mechanism should be ineffective in $[CH(AsF_5)_y]_x$, because of the much weaker spin–orbit interactions at the As atoms, which are highly shielded by the F atoms coordinated to them. Thus published data[74] demonstrate directly the importance of the effects of localisation in in $(CHI_y)_x$ and $(CHBr_y)_x$.

There are much fewer experimental data on the magnetic properties of PA doped with donors. The most important results are those obtained[76] by EPR *in situ* in the liquid-phase doping of thin films of *trans*-PA using a solution of sodium-benzophenone in THF. At low doping levels, the paramagnetic susceptibility of *trans*-$(N_yCH)_x$ remained practically constant, and differed little from that of non-doped *trans*-PA, but close to $y \simeq 0.05$ it increased sharply, accompanied by marked broadening of the EPR line and the appearance of temperature-independent χ_P. These data were interpreted[76] as proof of a first-order phase transformation at $y = y_c$ from a soliton lattice with zero density of states at the Fermi level $N(E_F)$ to a new quasi-metallic lattice, a "polaron metal", with a finite density $N(E_F)$. Such far-reaching conclusions appear doubtful, however, since there is insufficient information on the chemistry of the reactions in the PA–reducing agent system. Thus it has been established[77] that the solvation of Na^+ ions by THF has a marked influence on the width of the EPR line and the conductivity of specimens whose composition in the general case corresponds to the formula $[Na_y(THF)_z(CH)]_x$. At low values of y, solvation has a marked influence of σ, so that $\sigma_{z>0}/\sigma_{z=0} \simeq 10^4$, and with increase in y to 0.2, this ratio tends to 1; at low values of y for solvated Na^+ cations, $\Delta H < 1$ G, whereas for the non-solvated cations, $\Delta H \simeq 6$ G; at $y \simeq 0.01$, these ΔH values becomes equal.

Comparison of published conductivity and EPR data[77] also shows that there are strong interactions between the charge carriers and the local magnetic moments, that is the situation is analogous to that examined above for $(CHI_y)_x$; fairly strong spin–orbit scattering on the Na^+ ions should be expected. As a result, the paramagnetism of $(Na_yCH)_x$ should be determined by the simultaneous influence of several physical and chemical factors, among which the non-uniformity of the doping is of considerable importance. In Ref.76, the distribution of Na^+ was *a priori* regarded as uniform, but NMR data[78] show that even at y_{max}, the spectrum still contains a signal characteristic of non-doped PA.

In conclusion it may be noted that the absence of an EPR signal in the case of doped PA cannot be taken as evidence for the existence of spin-free solitons; for example, the same property is shown by chalcogenide and many other electrically conducting glasses.[38,75] In fact, the density $N(E_F)$ is most probably finite, but the electrons form pairs with antiparallel spins, so that the one-electron density of states $N(E_F)$ is equal to zero.

The reader interested in the detailed characteristics of non-crystalline solids is referred to published monographs.[38,75] It should be noted that the automatic transfer to disordered systems of ideas borrowed from classical band theory is not possible, and easily leads to artefacts.

V. OPTICAL PROPERTIES

The electronic absorption spectra of PA are completely typical of polyconjugated systems. The absorption bands of *cis*-PA has a clearly defined vibrational structure with maxima at 2.1, 2.3, and 2.4 eV, whose positions and intensities depend slightly on the previous history of the specimen. *cis–trans*-Isomerisation displaces the main maximum to 1.9 eV, and, as is often observed, to the disappearance of the vibrational structure.[79] By analogy with short polyenes, the absorption maximum can be assigned to a $\pi-\pi^*$ transition; the absorptivities, $\alpha \simeq 1.5 \times 10^5$ cm^{-1},[79] are characteristic of inter-band transitions in typical semiconductors.

After doping, the absorption band characteristic of the original PA becomes weaker, and is replaced by a new very broad structureless band at 0.5–0.9 eV. Typical results obtained by electrochemical doping[80] are shown in Fig.6. The absorption close to 0.7 eV is characteristic of all doped forms of PA, and is therefore associated with the electronic structure of the PA framework. Since the position of the new band corresponds approximately to the half-width of the band gap in the spectrum of the original PA, in the SSH model this band is called the "absorption in the middle of the gap". In addition, doping leads to the appearance in the infrared range of three strong bands at 0.17, 0.16, and 0.11 eV, whose positions are practically independent of the type of dopant, but are sensitive to the isotopic composition of the PA.[81]

The optical characteristics of PA have been discussed in detail.[19] It may be noted that in the SSH theory and its modifications, the spectrum of doped PA is determined by the characteristic vibrations of the charged solitons; the interaction of the solitons with π-electrons is accompanied by the appearance of new vibrational modes, three of which should be active in the infrared (IR) range. The IR absorption is described equally well by introducing topological defects of not the soliton type (C_{2v} symmetry) but the polaron type (C_{2h} symmetry). Particular attention has been paid to the absorption at about 0.7 eV, associated with the appearance of localised soliton levels exactly in the middle of the gap. Calculations[19] show that the appearance of a soliton in the PA chain should lead to the suppression of direct inter-band transitions, and the intensity of the transitions between the soliton levels should increase with increase in y as far as y_c, after which saturation should take place as a result of the overlap of these levels and the formation of a soliton band. The last conclusion, however, does not agree with experimental data,[33,36] according to which the optical density at 0.7 eV is proportional to the equilibrium concentration of the PA–dopant complex. The IR absorption data[82] also show a regular decrease in the transmission with increase in y as far as y_{max}.

The view that doping produces conjugation defects of different types is entirely reasonable. It is obvious, however, that the optical absorption can hardly be determined by the mobility of these defects; the broken bonds in three-dimensional inorganic amorphous semiconductors also give states situated "within the gap", but these states are not soliton states.[38] Thus the absorption spectra cannot serve as a test for solitons. A clear example is provided by a paper[83] whose authors reject completely the concept of conjugation defects, and attribute the "absorption within the gap" to charge transfer; a donor dopant adds an electron to the conductivity band, and an acceptor dopant generates a hole in the valence band. The conclusion that

there is alternation of the bonds in the PA chain is preserved completely, and the absorption is attributed to electromagnetic interactions between neighbouring chains. If however account is taken of the non-uniform distribution of the dopant, then the "absorption within the gap" can be directly related to an optical dielectric anomaly, characteristic of granulated metals. In this connection it may be noted that the maximum close to 0.7 eV, which is clearly defined in the reflectance spectra of $(CHI_y)_x$ films, disappears after the films have been compressed (unlike the other maxima in the IR range), and are replaced by a reflectance edge.[84] This phenomenon is readily explained in terms of the composite structure of doped PA using the familiar Maxwell–Harnett theory,§ but cannot be understood in terms of soliton models.

The charge-transfer model also provides an extremely effective interpretation of the three IR bands of doped PA; they are attributed to the interaction of the stretching vibrations of the framework with charge oscillations in a partly oxidised or reduced segment of the polymer; this is analogous to the situation for charge-transfer complexes based on TCNQ.[85] On the other hand, the IR spectra of β-carotene, which is an appropriate model compound with eleven conjugated bonds, are completely analogous to the spectrum of PA.[81,86] Thus published data[81,84–86] indicate that the optical absorption in PA is molecular in character. Quantum-chemical calculations of the electronic and vibrational structure[87,88] of model oligomeric radical-cations $C_{2n}H_{2n+2}^{+}$, cations $C_{2n+1}H_{2n+3}^{+}$, and dications $C_{2n}H_{1n+2}^{2+}$ [87,88] show that species of all three types are capable of contributing to the observed absorption. Moreover, the calculation[88] predicts intensive absorption close to 0.7 eV for β-carotene or PA doped with donors, with the formation of radical-anions $C_{2n}H_{2n+2}^{\cdot-}$; subsequent measurements[89] showed complete agreement with these predictions.

VI. PROBABLE MECHANISMS OF CONDUCTIVITY

An understanding of the mechanisms of charge transfer is hardly possible without taking account of the real structure of PA. The very complex morphology of PA was discussed above. Although the degree of crystallinity of the specimens reaches 80%, the average size of the crystallites is small, and does not exceed several nm.[90] The disorientation of the crystallites and the scatter in their sizes and shapes makes the direct determination of the crystal structure impossible; the diffraction patterns of PA seldom contain more than ten reflections, so that the crystallographic parameters have to be selected by a combined analysis of the diffraction patterns and calculations of the crystal packing.[25] The crystalline phase coexists with an amorphous phase; measurements of the thermo-stimulated creep[91] show that PA contains both amorphous volumes and thin inter-phase layers, separating the crystallites. It cannot be assumed that the general nature of the packing of the macromolecules in the amorphous phase differs significantly from that in the crystalline phase; the maxima of the diffuse scattering on the diffraction patterns coincide with the position of the principal reflection, but in the amorphous phase the concentration of packing defects (folds and twists in the chains, vacancies, etc.) is increased.

The diffraction patterns, however, are insensitive to local molecular defects, which to a large extent determine the charge transfer. The defects due to the presence in PA of sp^3-hybridised C atoms are particularly important. Acording to NMR and DPN data,[92,93] their concentration amounts to several percent. The presence of C(sp^3) atoms naturally breaks the conjugation chains. The Raman spectra, which provide a unique source of information on the magnitude of $N_{C=C}$,[94] show that, usually, not more than 20% of the chains have $N_{C=C} \geqslant 20$.

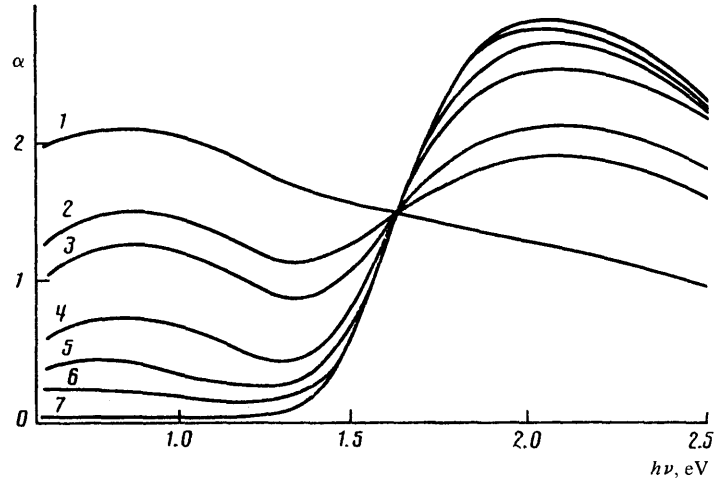
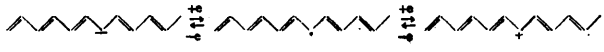


Figure 6. Absorption spectra of $[Ch(ClO_4)_y]_x$ at different levels of electrochemical doping[80] for y = 0.078 (*1*), 0.047 (*2*), 0.027 (*3*), 0.012 (*4*), 0.0065 (*5*), 0.003 (*6*), 0 (*7*).

§ See, for example, L.Genzel and U.Kreiberg, Z.Phys., 1980, **37**, 93.

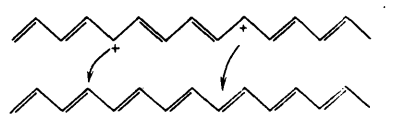
The macroscopic resistance of PA is apparently determined by a large number of factors (see section III). The indeterminacy associated with the disordered nature of the PA structure is so great that it is possible to construct only phenomenological models of charge transfer. When the real structure of PA is taken into account, it immediately becomes obvious that charged solitons or polarons cannot be responsible for the macroscopic conductivity; since they are topological conjugation defects, they can move only within the continuous conjugation segments. These segments are comparatively small, however, and the value of σ for doped PA is not related to the value of N_{C-C}; the electrical and magnetic properties of doped and non-doped PA are practically independent of the molecular mass in the range $400 \leqslant M_n \leqslant 920\,000$.[11] The results of studies of copolymers of acetylene with carbon monoxide,[95] where the mole fraction of CO was varied in the range 5–13%, are even more convincing. In these copolymers, the conjugation chain is frequently interrupted by $-C(=O)-$ units, so that $6 < N_{C-C} < 20$, yet the electrical properties of the doped and non-doped copolymers are the same as the corresponding properties of PA. The expected results were obtained from numerical calculations using the SSH model,[96] according to which the $-C(=O)-$ group in the *trans*-PA chain acts as a trap for neutral or negative solitons, and as a repulsion barrier for positive solitons.

For weakly doped ($y \lesssim 0.005$) *trans*-PA, Kivelson[97] proposed a mechanism of charge transfer by inter-soliton jumps. Every time a mobile soliton $S^{\cdot}$ passes close to a charged soliton $S^{\pm}$ which is bound by Coulombic attraction to an ion of the dopant and is therefore immobile, isoelectronic hopping of an electron to a neighbouring chain becomes possible:



Measurements of macroscopic characteristics, namely the frequency–temperature dependence of σ [98] and the $\sigma(T)$ relationships at different pressures,[99] agree well with the predictions,[97] but more detailed experiments on the influence of magnetic fields on the mobility of the carriers[100] gave results which contradicted the Kivelson model. In fact, the Kivelson mechanism is realistic only when the following requirements are satisfied simultaneously: 1) N_{C-C} should be very large, so that the solitons $S^{\cdot}$ can move along the chain without hindrance; 2) most of the chains should contain $S^{\cdot}$; and 3) the dopant should be distributed uniformly. From the previous sections it is clear that none of these requirements is in fact satisfied.

The corner-stone of the soliton concept is the assumption that the ground state of the chain is degenerate. The model of Ref.97 is obviously inapplicable in principle to either *cis*-PA or other conducting polymers. A different model[101] claiming to explain the mechanisms of conductivity in all doped polymers assumes interchain charge transfer by the correlated jumps of bipolarons:



The model of Ref.101 is designed primarily to explain spin-free charge transfer, and its experimental basis is the apparent absence of paramagnetism in doped PA. A semiquantitative calculation using this model reproduces only the general course of the $\sigma(y)$ relationship; so many assumptions, simplifications, and fitting parameters are used, however, that the agreement with experiment appears artificial. The greatest objections can be made to the actual idea of high-temperature jumps of bipolarons between the chains; by definition, the bipolarons in PA are not simply charged quasi-particles but topological defects in intramolecular chemical bonds. For this reason, the bipolaron model of Ref.101 can be regarded as an artefact, and its indvidual aspects will not be examined in detail.

It has been pointed out many times that the general character of the $\sigma(T)$ relationships for PA is similar to that of the typical relationships for doped inorganic amorphous semiconductors. This is why efforts are made to explain the electrical properties of PA using ideas based on jump mechanisms. For disordered systems, a unique role is played by $\sigma(T)$ measurements using alternating current. To ensure macroscopic conductivity using direct current or at low frequencies, the carriers must pass through the entire specimen; in a disordered system, this is possible only when there is a percolation network. At sufficiently high frequencies, percolation considerations are directly inapplicable, and the movement of the carriers reduces to jumps back and forward between two neighbouring localised states. This situation can be described by the so-called pair approximation.[75] A corresponding model for PA was proposed by Summerfield,[102], whose calculations adequately reproduce the static and frequency $\sigma(T)$ relationships, including the imaginary part of the complex conductivity, which is not consistent with the Kivelson model, and provide a qualitative description of the evolution of the density of states close to the Fermi level during doping. It should be emphasised that the Summerfield model does not contain assumptions about the nature of the states between which the jumps take place, in particular about their mobility, and at the same time reproduces the experimental data[98] more effectively than the Kivelson model.[97]

The electrical properties of moderately and highly doped PA are best described by the model of Sheng,[103] which was initially developed for granulated metals and which assumes the formation in PA of quasi-metallic clusters separated by narrow potential barriers—the non-doped PA regions. The movement of the carriers between the clusters takes place by tunnelling at low temperatures, and by thermally activated jumps at high temperatures. Thus detailed measurements[104] show a gradual decrease in the strength of the characteristic Mott relationship $\sigma \sim \exp(-T^{-1/4})$ when PA, moderately doped with AsF_5, is cooled to a temperature below 16 K; in the range $0.03\ \text{K} < T < 1\ \text{K}$, the conductivity of highly doped $[Ch(AsF_5)_{0.1}]_x$ becomes independent of temperature.[105] This behaviour cannot be explained without using tunnelling concepts.

Measurements of the temperature, field, and frequency dependence of the conductivity, and thermo-EMF measurements,[106] also show excellent agreement with Sheng's theory. The most convincing proof is apparently provided by the experiments of Refs.49 and 50 (see Fig.5); highly doped PA is in fact a system of non-combined quasi-metallic clusters. In this cluster model, the superposition of two main transfer mechanisms can be proposed. In one limiting case, the movement of the carriers is similar to the movement of the electrons in a metal, that is the interaction with the lattice is relatively weak, and the carriers have a high mobility and a comparatively long mean free path. In the other limiting case, the interaction with the lattice is strong, and the carriers have a very short mean free path and a low mobility. Within the clusters, the carriers probably move as a wave packet. Thus at a temperature below the Debye temperature, they may move as non-localised polarons of small radius in a narrow energy band, and at a temperature above the Debye temperature, the carriers move by jumps. This model is attractive, particularly since in polymers the Debye temperature is not strictly defined, and in fact there may be a distribution of Debye temperatures. Estimation of the drift mobility of the carriers μ, which is defined as the average rate of movement of the current carrier in the direction of the field and which is therefore a macroscopic characteristic, using the simple equation (3), gives for weakly doped PA the value $\mu = 5 \times 10^{-5}\ \text{cm}^2\ \text{V}^{-1}\ \text{s}^{-1}$.[39] As shown by Ioffe,[107] the average mean free path L of a carrier with an

effective mass m^* at ordinary temperatures is given by the expression $L \simeq 10^{-8}\ \mu(m^*/m_0)^{1/2}$, where m_0 is the mass of the free carrier. Assuming that the order of magnitude of the ratio m^*/m_0 is close to 1 gives for weakly doped PA the value $L \simeq 10^{-5}$ Å. This is many orders of magnitude smaller than the lattice constant a, so that the concepts of mean free path or mobility lose their significance. For highly doped PA, Eqn.(3) gives $\mu = 1\ cm^2\ V^{-1}\ s^{-1}$;[39] Ioffe's equation gives $L \simeq 1$ Å, which is also unlikely.

Dielectric measurements at high frequencies of $1.5-5\ cm^{-1}$ [108] revealed a high microscopic mobility (see Table), however, and it was concluded that the frequency dependence of the conductivity can be described by the superposition of two mechanisms. The first is due to free carriers, the absorption on which is described by the Drude relationship, and the second is associated with carrier jumps with the participation of phonons between microscopic states. At the microscopic level, these states are localised, so that the conductivity for direct and alternating current can be examined successfully using jump models.

Electrophysical characteristics of doped PA (accuracy of the determination ±25%).[108]

Specimen	n, cm^{-3}	τ, ps	μ, $cm^2\ V^{-1}\ s^{-1}$	σ, $\Omega^{-1}\ cm^{-1}$
trans-$(CHI_{0.011})_x$	$1.1\cdot10^{15}$	2.7	$3.7\cdot10^3$	0.5
trans-$[CH(AsF_5)_{0.011}]_x$	$5.0\cdot10^{15}$	10.0	$15.0\cdot10^3$	9.5

Notation: n and τ are the concentration and the mean free path of the current carriers μ the mobility of the carriers, and σ the specific conductance.

VII. THE STRUCTURE OF THE CONDUCTING PHASE

In a first approximation, doped PA can apparently be regarded as a composite containing two phases: non-doped and doped to saturation. In principle, depending on the previous history of the specimens, the volume fraction of the conducting phase can vary in the range $0 \leqslant f \leqslant 1$. The limiting cases correspond to the hypothetical single crystals, and in real specimens, some intermediate situation is established. This interpretation can be justified by the following experimental data.

1. In the absorption spectra there is an isosbestic point,[35,36,80] indicating the existence of only two states in PA–dopant systems, irrespective of the doping level (Fig.6).

2. Periodic recording of the diffraction patterns during doping always show a gradual decrease in the intensities of the reflections from the original PA, and the appearance of a new set of reflections. No signs of intermediate structures are detected.[109-111]

3. The reduced volume of the PA specimens is linearly dependent on the concentration of the dopant.[112]

Analysis of the experimental data indicates that the electron-conducting structures are formed first in the amorphous phase of PA. In fact, the first signs of the doped phase on the diffraction patterns appear only at $y \geqslant 0.02$; at $0 < y < 0.02$, only an increase in the intensity of the background scattering due to the adsorption of iodine on the PA surface was observed.[110] The swelling of the specimens during doping becomes appreciable only at $y \geqslant 0.05$.[112] The main increase in σ, however, takes place at $y \lesssim 10^{-2}$ (Fig.3). On doping with iodine from the gas phase, σ increases by five orders of magnitude in a time $t = 10^3$ s, and is saturated after $t = 10^4$ s, and both σ_{max} and the value of t at which it is reached are completely independent of the thickness of the PA films, which in the experiments of Ref.47 was varied from 5×10^{-6} cm to 10^{-2} cm.

At the same time it follows from kinetic data[47] that the diffusion of iodine in PA is very slow, with a coefficient $10^{-14}-10^{-13}\ cm^2\ s^{-1}$. Even for the small non-solvated Li^+ ion, the diffusion coefficient in PA is $\sim10^{-13}\ cm^2\ s^{-1}$ at 356 K.[113] These values are typical of solid-state diffusion. Thus the depth of the diffusion according to Fick's law $l_D = (2Dt)^{1/2}$ is ~0.1 μm at $t = 10^3$ s, which appears unlikely. It is known, however, that the diffusion coefficient along the grain boundaries in polycrystalline specimens is many times greater, and the activation energy of diffusion significantly lower, than in the volume of the granule. Moreover, it has been found[35,37] that the mass of the specimens in I_2 vapour increases rapidly at $t \leqslant 10$ s, and only at $10\ s < t < 10^4$ s, increases according to a t^n law, where $1/3 < n < 1/2$, indicating solid-state diffusion.

The combined data on the distribution profiles of the dopants and the kinetics of doping lead to the following picture. In the rapid first stage, the entire external surface of PA is covered with a monolayer of the dopant. In the slower second stage, the dopant diffuses into the amorphous phase, occupying the spaces between the crystallites. In the third stage, the dopant diffuses into the crystallites, and a new crystalline phase is formed. This picture is consistent with the morphology of PA and with the established $\sigma(y)$ relationships, without introducing doubtful assumptions about the uniform distribution of the dopant. The sharp increase in σ close to y_c (Fig.4) is naturally attributed to percolation, which takes place when the electrically conducting structures are formed in the space between the crystallites; the subsequent increase in f does not make a significant contribution to the macroscopic conductivity. In fact, the high conductivity is not determined by high crystallinity, since doping amorphous PA with iodine gives the same value of σ_{max} as doping highly crystalline specimens.[114]

The question of how the conducting phase of PA is "constructed" can be examined. The conductivity mechanisms which were examined above and which provide an adequate description of the electrical properties of PA are completely indifferent to the specific structure of the localised states or quasi-metallic clusters. There is apparently no particular need to assume that doped conjugated polymers differ fundamentally from the familiar low-molecular-weight charge-transfer complexes (CTC) of the TTF–TCNQ type.[2] In the last case, before the formation of the CTC, the electron clouds of the donor and the acceptor are closed, and when the molecular crystal is formed, extensive charge transfer takes place, converting the crystal to the quasi-metallic state; the initially completely full band becomes half-filled. It may be said that in this case, TCNQ is "doped" by TTF or vice versa, so that the concepts of "dopant" and "matrix" can be interchanged.

From this viewpoint, doped PA represents a particular case of systems of the TTF–TCNQ type with a low and varying concentration of donor or acceptor molecules. The optimum magnitude of the charge transfer is 0.5–0.8 e.[115] This is possible either with partial charge transfer or when a CTC with stoichiometry different from 1:1 is formed. In PA, both situations are probably realised; the first may be characteristic of chemical doping, and the second of electrochemical doping, when the dopant is only a source of counterions preserving the electrical neutrality of PA. The role of donors or acceptors in PA is played by conjugated segments of varying length, bounded by defects in the molecular structure.

The basic principle of supermolecular organisation, ensuring high conductivity, is well known; it is necessary to have a non-stratified bifilar type of packing, where the donors and acceptors crystallise in regular isolated stacks, within which mixed valence states are produced, and the movement of the carriers takes place by a so-called

relay mechanism.[2] The individual details of this mechanism as applied to conducting polymers have been discussed by Wegner.[116] Two models of the packing in doped PA have now been developed on the basis of the diffraction patterns and calculations. The first model [25] assumes structural analogies with intercalated graphite; the acceptor molecules are introduced between the close-packed planes of PA. In the resulting layer structures, the transfer of the carriers should take place chiefly within the partly oxidised planes of PA, and should be quasi-two-dimensional in character. It is noteworthy that this model is unsuitable for interpreting the diffraction patterns of PA doped with alkali metals. For these complexes, a quasi-one-dimensional structure is assumed, in which the metal ions occupy channels in the tetragonal lattice formed by four parallel PA chains.[25] If the analogy with graphite is retained, however, there are no grounds for expecting such significant differences between the structures of the various complexes.

On the other hand, it follows even from a previous analysis[110] that the diffraction patterns for $(CHI_y)_x$ are consistent not only with the intercalation model. In an alternative model, the dopant is introduced between PA layers in which the planes of the macromolecules are arranged normal or almost normal to the plane of the layer. The relationship between the two models is illustrated schematically in Fig.7. The analogy between the second model[110,116] and the packing of low-molecular-weight CTC and radical-ion salts of TCNQ is obvious. The most convincing evidence in support of this type of packing was recently obtained in a diffraction analysis of highly oriented films of *trans*-$[CH(SbF_6)_y]_x$.[116] The crystal structure can be represented as the superposition of two incommensurable sub-lattices: the first is formed by the PA chains, and the second by the SbF_6^- ions. The second lattice is hexagonal and disordered along the crystallographic direction coinciding with the axes of the PA macromolecules. The distance between neighbouring PA segments forming the stacks is 3.44 Å, which ensures effective interaction between the π-electrons. In this model, the PA segments reduced or oxidised to radical-ions are stabilised by complex formation with neighbouring neutral segments according to the scheme

$$(CH)_n^{\pm\cdot} + (CH)_n \rightleftarrows [(CH)_n\,(CH)_n]^{\pm\cdot}$$

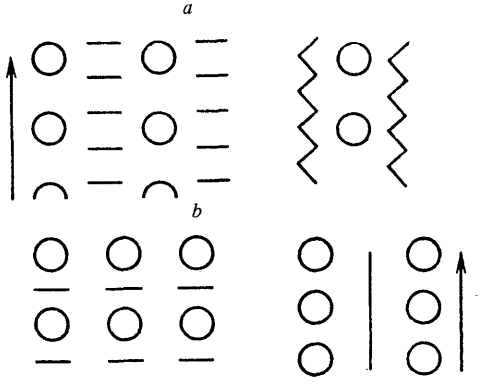


Figure 7. Probable crystal packing in doped PA (on the left—projection along the PA chain direction, on the right—projection at right angles to the PA chain direction): *a*) quasi-one-dimensional model,[116] *b*) quasi-two-dimensional model;[25] the arrows show the preferred direction of charge transfer; the circles represent the dopant, and the dashes the end faces of the planar PA chains.

It follows directly from this scheme that the complex formation is possible not only in the crystalline phase but in all cases where a minimum of two PA segments are arranged relative to one another in such a way that charge transfer is possible between them. These complexes are apparently acceptable as the prototype of the localised states; their concentration increases with increases in y, and they merge at any $y = y_c$. It is appropriate to recall that the packing of the macromolecules in the amorphous phase differs little from that in the crystallites. According to the appropriate comparison made in Ref.117, the local structure of the rigid-chain polymers is more like the packing of raw spaghetti in a partly filled box than the packing of cooked spaghetti in a pan. This makes clear the importance in amorphous polymers of the intermolecular interactions which stabilise the quasi-metallic state and which make possible the existence of conducting clusters of appreciable dimensions.

The "metallic character" of the clusters, revealed by the different slopes of the curves in Fig.5, is variable, and depends on the dopant. In "physical" soliton models, dopants of the same type (for example acceptors) are not distinguished. For chemists, the different electrophysical properties of PA—dopant complexes can be attributed to the difference in the degree of charge transfer and the difference in the stability constants of the CTC (see section III). The most stable complexes are probably formed in the reaction of PA with AsF_5, which is a very strong Lewis acid. The correctness of these arguments is apparently confirmed by the data of Ref.108, given in the Table.

- - - o0o- - -

From the extensive range of fundamental problems relating to PA, as before, the question of the nature of the conductivity is attracting the greatest attention. There arises the question of whether solitons (or polarons) are physically real, or merely an elegant but artificial method of description. The answer to this question is important not only for theoreticians. The development of new materials of practical importance can hardly be achieved without a detailed understanding of the electronic processes responsible for their properties. A complete understanding has obviously not yet been reached. The chemistry and physics of macromolecular "synthetic metals", of which PA is the prototype, still appear as a mosaic, and considerable efforts are required to establish a clear and consistent picture.

Nevertheless, the information which has already accumulated up to the present provides some possibilities for generalisation. According to the familiar Occam's principle, entities are not to be multiplied beyond necessity. In accordance with this principle, the present authors consider that the principal properties of PA and its analogues can be examined using more traditional non-soliton approaches. The soliton concept, however, has provided an exceptionally effective stimulus for theoretical and experimental studies which might not have been carried out in a different situation. This has led to a better understanding of the entire set of relationships between the structure and properties of matter—one of the cardinal problems of present-day chemistry.[118]

REFERENCES

1. I.F.Shchegolev, Phys.Status Solidi, 1972, **A12**, 9.
2. V.S.Starodub and I.V.Krivoshei, Uspekhi Khim., 1982, **51**, 764 [Russ.Chem.Rev., 1982(5)].

3. A.A.Berlin, M.A.Kheiderikh, B.E.Davydov, et al., "Khimiya Polisopryazhennykh Sistem" (The Chemistry of Non-conjugated Systems), Izd.Khimiya, Moscow, 1972.
4. Ya.M.Paushkin, T.P.Vishnyakova, A.F.Lunin, and S.A.Nizova, "Organicheskie Polimernye Poluprovodniki" (Organic Polymeric Semiconductors), Izd.Khimiya, Moscow, 1971.
5. H.Shirakawa, E.J.Louis, A.G.McDiarmid, C.K.Chiang, and A.J.Heeger, J.Chem.Soc.Chem.Comm., 1977, 578.
6. V.Engelmann, G.Lieser, W.Müller, and G.Wegner, Angew. Makromol.Chem., 1981, **94**, 105.
7. C.R.Fincher, C.-E.Chen, A.J.Heeger, A.G.McDiarmid, and J.B.Hastings, Phys.Rev.Lett., 1982, **48**, 100.
8. J.C.W.Chien, F.E.Karasz, and K.Shimamura, Makromol. Chem.Rapid Comm., 1982, **3**, 655.
9. C.S.Yannoni and T.C.Clarke, Phys.Rev.Lett., 1983, **51**, 1191.
10. M.J.Duijvestijn, A.Manenschijn, J.Smidt, and R.A.Wind, J.Magn.Reson., 1985, **64**, 461.
11. J.C.W.Chien, J.M.Warakomski, F.E.Karasz, and M.A.Schen, Macromolecules, 1985, **18**, 2380.
12. P.Bernier, S.Lefrant, M.Rolland, M.Aldissi, M.Galtier, A.Montaner, C.Linaya, and F.Schue, J.Electron.Mater., 1983, **12**, 289.
13. T.Ito, H.Shirakawa, and S.Ikeda, J.Polym.Sci.: Polym.Chem. Ed., 1974, **12**, 11.
14. W.P.Su, J.R.Schrieffer, and A.J.Heeger, Phys.Rev., 1980, **B22**, 2099.
15. S.A.Brazovskii, Pis'ma v Zhur.Eksp.Teor.Fiz., 1978, **28**, 656.
16. J.L.Brédas, R.R.Chance, and R.Silbey, Phys.Rev., 1982, **B26**, 5843.
17. A.R.Bishop, D.K.Campbell, and K.Fesser, Mol.Cryst.and Liquid Cryst., 1981, **77**, 253.
18. G.Grella, F.Mancini, M.Marinaro, and G.Scarpetta, Phys. Lett., 1984, **A100**, 482.
19. H.W.Streitwolf, Phys.Status Solidi, 1985, **B127**, 11.
20. A.G.MacDiarmid and A.J.Heeger, Synth.Met., 1979/80, **1**, 101.
21. J.C.W.Chien, J.M.Warakomski, F.E.Karasz, W.L.Chia, and C.P.Lillya, Phys.Rev., 1983, **B28**, 6937.
22. G.Mihály, G.Vancsó, S.Pekker, A.G.S.Jánossy, Synth.Met., 1979/80, **1**, 357.
23. D.Moses, A.Denenstein, J.Chen, A.J.Heeger, P.McAndrew, T.Woerner, A.G.McDiarmid, and Y.W.Park, Phys.Rev., 1982, **25**, 7652.
24. S.Ikehata, J.Kaufer, T.Woerner, A.B.Pron, M.A.Druy, A.Sivak, A.J.Heeger, and A.G.McDiarmid, Phys.Rev.Lett., 1980, **45**, 1123.
25. R.H.Baughman, N.S.Murthy, G.G.Miller, et al., J.Phys. (France): Colloq., 1983, **77**, 185.
26. M.Aldissi and F.Schué, Solid State Comm., 1984, **50**, 885.
27. A.G.S.Jánossy, L.Pogány, S.Pekker, and R.Swietlik, Mol.Cryst.and Liquid Cryst., 1981, **77**, 185.
28. J.P.Louboutin and F.Beniere, J.Phys.and Chem.Solids, 1982, **43**, 233.
29. A.B.Prón, A.G.McDiarmid, and A.J.Heeger, Synth.Met., 1984, **9, 115.**
30. T.Matsuyama, H.Sakai, M.Yamaoka, Y.Maeda, and H.Shirakawa, J.Phys.Soc.Jap., 1983, **52**, 2238.
31. M.Tokumoto, H.Oyanagi, T.Ishiguro, H.Shirakawa, H.Nemoto, T.Matsushita, M.Ito, H.Kuroda, and K.Kohra, Solid State Comm., 1983, **48**, 861.
32. L.R.Anderson, G.P.Pez, and S.L.Hsu, J.Chem.Soc.Chem. Comm., 1978, 1066.
33. P.Brant and D.C.Weber, J.Polym.Sci.: Polym.Chem.Ed., 1983, **21**, 1929.
34. B.McQuillan, G.B.Street, and T.C.Clarke, J.Electron.Mater., 1982, **11**, 471.
35. J.Kanicki, E.Vander Donckt, and S.Boué, J.Chem.Soc. Faraday Trans.II, 1981, **77**, 2157.
36. J.Kanicki, S.Boué, and E.Vander Donckt, Thin Solid Films, 1982, **92**, 243.
37. M.Rolland, S.Lefrant, M.Aldissi, P.Bernier, E.Rzepka, and F.Schué, J.Electron.Mater., 1981, **10**, 619.
38. N.F.Mott and E.A.Davies, "Electronic Processes in Non-crystalline Substances" (Translated into Russian), Izd.Mir, Moscow, 1982.
39. Y.-W.Park, A.J.Heeger, M.A.Druy, and A.G.MacDiarmid, J.Chem.Phys., 1980, **73**, 946.
40. C.K.Chiang, Y.W.Park, A.J.Heeger, H.Shirakawa, and E.J.Louis, J.Chem.Phys., 1978, **69**, 5098.
41. Y.W.Park, J.C.Woo, K.H.Yoo, W.K.Han, C.H.Choi, T.Kobayashi, and H.Shirakawa, Solid State Comm., 1983, **46**, 731.
42. E.K.Sichel, M.F.Rubner, and S.K.Tripathy, Phys.Rev., 1982, **B26**, 6719.
43. J.C.W.Chien, Y.Yamashita, J.A.Hirsch, J.L.Fan, M.A.Schen, and F.E.Karasz, Nature, 1982, **299**, 608.
44. B.Wessling, Makromol.Chem., 1984, **185**, 1265.
45. J.H.Edwards, R.Fisher, and B.Vincent, Makromol.Chem. Rapid Comm., 1983, **4**, 393.
46. I.Kminek and J.Trekoval, Makromol.Chem.Rapid Comm., 1984, **5**, 423.
47. H.Kiss, W.H.Meyer, D.Baeriswyl, and G.Harbeke, J.Electron. Mater., 1980, **9**, 763.
48. L.B.Coleman, Rev.Sci.Instrum., 1978, **49**, 58.
49. M.Wan, P.Wang, Y.Cao, R.Qian, F.Wang, X.Zhao, and Z.Gong, Solid State Comm., 1983, **47**, 759.
50. K.Kume, S.Masubuchi, Y.Mochizuki, Y.Hiroyama, K.Mizoguchi, and K.Mizuno, Solid State Comm., 1986, **58**, 473.
51. B.R.Weinberger, E.Ehrenfreund, A.Pron, A.J.Heeger, and A.G.McDiarmid, J.Chem.Phys., 1980, **72**, 4749.
52. I.B.Goldberg, H.R.Crowe, P.R.Newman, A.J.Heeger, and A.G.McDiarmid, J.Chem.Phys., 1979, **70**, 1132.
53. M.Nechtschein, F.Devreux, F.Genoud, M.Guglielmi, and K.Holczer, J.Phys.(France): Colloq., 1983, **44**, C3–209.
54. S.Kuroda, M.Tokumoto, N.Konoshita, T.Ishiguro, and H.Shirakawa, J.Phys.(France): Colloq., 1983, **44**, C3–303.
55. H.Thomann, H.Kim, A.Morrobel-Sosa, L.R.Dalton, M.T.Jones, B.H.Robinson, T.C.Clarke, and Y.Tomkiewicz, Synth.Met., 1984, **9**, 255.
56. L.R.Dalton, H.Thomann, A.Morrobel-Sosa, A.Chiu, M.E.Galvin, G.E.Wnek, Y.Tomkiewicz, N.S.Shiren, B.H.Robinson, and A.L.Kwiram, J.Appl.Phys., 1983, **54**, 5583.
57. S.Kuroda, H.Bando, and H.Shirakawa, Solid State Comm., 1984, **52**, 893.
58. H.Thomann, L.R.Dalton, M.Grabowski, and T.C.Clarke, Phys.Rev., 1985, **31**, 3141.
59. N.S.Shiren, Y.Tomkiewicz, H.Thomann, L.R.Dalton, and T.C.Clarke, J.Phys.(France): Colloq., 1983, **44**, C3–223.
60. F.Masin, G.Gusman, and R.Deltour, Solid State Comm., 1981 **39**, 505.
61. W.G.Clark, K.Glover, G.Mozurkewicz, C.T.Murayama, J.Sanny, S.Etemad, and M.Maxfield, J.Phys.(France): Colloq., 1983, **44**, C3–239.
62. P.K.Kahol, M.Mehring, and X.Wu, J.Phys.(France), 1985, **46**, 1683.
63. M.Mehring, H.Seidel, W.Müller, and G.Wegner, Solid State Comm., 1983, **45**, 1075.
64. G.Voelkel, S.A.Dzuba, A.Bartl, W.Brunner, and J.Froehner, Phys.Status Solidi, 1984, **A85**, 257
65. B.R.Weinberger, J.Kaufer, A.J.Heeger, A.Pron, and A.G.McDiarmid, Phys.Rev., 1979, **B20**, 223.

66. Y.Tomkiewicz, T.D.Schultz, H.B.Broom, T.C.Clarke, and G.B.Street, Phys.Rev., 1981, **B24**, 4348.
67. J.C.W.Chien, J.M.Warakomski, and F.E.Karasz, J.Chem. Phys., 1985, **82**, 2118.
68. K.Kume, K.Mizuno, K.Mizogushi, et al., J.Phys.(France): Colloq., 1983, **44**, C3–353.
69. D.Davidov, S.Roth, W.Neumann, and H.Sixl, Z.Phys., 1983, **B51**, 145.
70. N.Tokumoto, N.Kinoshita, S.Kuroda, T.Ishiguro, H.Shirakawa, and H.Nemoto, J.Phys.(France): Colloq., 1983, **44**, C3–299.
71. A.J.Epstein, H.Rommelmann, M.A.Druy, A.J.Heeger, and A.G.McDiarmid, Solid State Comm., 1981, **38**, 683.
72. M.Peo, S.Roth, K.Dransfeld, and J.Hocker, "Physics in One Dimension" (Edited by J.Bernasconi and T.Schneider), Springer, 1981, p.218.
73. A.Bartl, H.-G.Doege, J.Froehner, G.Lehmann, and B.Pietrass, Synth.Met., 1984/85, **10**, 151.
74. D.Davidov, S.Roth, W.Neumann, and H.Sixl, Solid State Comm., 1984, **52**, 375.
75. V.L.Bonch-Bruevich, I.P.Zvyagin, R.Kaiper, et al., "Elektronnaya Teoriya Neuporyadochennykh Poluprovodnikov" (The Electronic Theory of Disordered Semiconductors), Izd.Nauka, Moscow, 1981.
76. F.Moraes, J.Chen, T.C.Chung, and A.J.Heeger, Synth.Met., 1985, **11**, 271.
77. C.Mathis and B.Francois, Synth.Met., 1984, **9**, 347.
78. I.Heinmaa, M.Alla. A.M.Vainrub, et al., "Materialy VI Vsesoyuznogo Soveshchaniya po Probleme 'Kompleksy s Perenosom Zaryada i Ion-radikal'nye Soli'" (Proceedings of the Sixth All-Union Conference on Charge-transfer Complexes and Radical-ion Salts), Izd.Inst.Khim.Fiz.Akad.Nauk SSSR, Chernogolovka, 1984, p.112
79. H.Fujimoto, K.Kamiya, J.Tanaka, and M.Tanaka, Synth.Met., 1985, **10**, 367.
80. A.Feldblum, J.H.Kaufman, S.Etemad, A.J.Heeger, T.C.Chung, and A.G.McDiarmid, Phys.Rev., 1982, **B26**, 815.
81. I.Harada, Y.Furukawa, M.Tasumi, H.Shirakawa, and S.Ikeda, J.Chem.Phys., 1980, **73**, 4746.
82. C.Benoit, O.Bernard, M.Palpacuer, M.Rolland, and M.J.M.Abadie, J.Phys.(France), 1983, **44**. 1307.
83. A.J.Glick, Phys.Rev.Lett., 1982, **49**, 804.
84. W.Markowitsch, F.Kuchar, K.Seeger, and S.Roth, Solid State Comm., 1984, **51**, 271.
85. J.F.Rabolt, T.C.Clarke, and G.B.Street, J.Chem.Phys., 1982, **76**, 5781.
86. J.P.Devlin, J.Phys.Chem., 1982, **86**, 3064.
87. T.Yamabe, K.Akagi, T.Yanabe, K.Fukui, and H.Shirakawa, J.Phys.Chem., 1982, **86**, 2359.
88. T.Yamabe, K.Akagi, T.Matsui, K.Fukui, and H.Shirakawa, J.Phys.Chem., 1982, **86**, 2365.
89. J.M.Dohan, S.Boué, and E.Vander Donckt, Nouv.j.chim., 1983, **7**, 161.
90. H.Haberkorn, H.Naarmann, K.Penzien, J.Schlag, and P.Simak, Synth.Met., 1982, **5**, 51.
91. T.Elsayed, J.Elhout, B.Francois, C.Mathis, D.G.Chatain, and C.Lacabanne, J.Phys.(France): Colloq., 1983, **44**, C3–131.
92. T.Terao, S.Maeda, T.Yamabe, K.Akagi, and H.Shirakawa, Chem.Phys.Lett., 1984, **103**, 347.
93. R.A.Wind, M.J.Duijvestijn, and J.Vriend, Solid State Comm., 1985, **56**, 713.
94. H.Kuzmany, Pure Appl.Chem., 1985, **57**, 235.
95. J.C.W.Chien and G.N.Babu, J.Chem.Phys., 1985, **82**, 441.
96. W.Förner, M.Seel, and J.J.Ladik, Solid State Comm., 1986, **57**, 463.
97. S.Kivelson, Phys.Rev., 1982, **B25**, 3798.
98. A.J.Epstein, H.Rommelmann, M.A.Abkowitz, and H.W.Gibson, Phys.Rev.Lett., 1981, **47**, 1549.
99. D.Moses, J.Chen, A.M.Denenstein, M.Kaveh, T.C.Chung, A.J.Heeger, A.G.McDiarmid, and Y.W.Park, Solid State Comm., 1981, **40**, 1007.
100. E.L.Frankevich, D.I.Kadyrov, I.A.Sokolik, and V.M.Kobryanskii, 1983, 1642.
101. R.R.Chance, J.L.Brédas, and R.Silbey, Phys.Rev., 1984, **B29**, 4491.
102. S.Summerfield, Phil.Mag., 1985, **B25**, 9.
103. P.Sheng, Phys.Rev., 1980, **B21**, 2180.
104. M.Audenaert, Phys.Rev., 1984, **B30**, 4609.
105. C.M.Gould, D.M.Bates, H.M.Bozler, A.J.Heeger, M.A.Druy, and A.G.McDiarmid, Phys.Rev., 1981, **B23**, 6820.
106. K.Ehinger and S.Roth, Phil.Mag, 1986, **B53**, 301.
107. A.F.Ioffe, Fiz.Tverd.Tela, 1953, **1**, 1.
108. L.Genzel, F.Kremer, A.Poglitsch, G.Bechtold, K.Menke, and S.Roth, Phys.Rev., 1984, **B29**, 4595.
109. M.Monkenbusch, B.S.Morra, and G.Wegner, Makromol. Chem.Rapid Comm., 1982, **3**, 69.
110. M.Monkenbusch, Makromol.Chem.Rapid.Comm., 1981, **3**, 601.
111. C.Riekel, H.W.Hässlin, K.Menke, and S.Roth, Synth.Met., 1984, **10**, 31.
112. B.Francois, N.Mermilliod, and L.Zuppiroli, Synth.Met., 1981, **4**, 131.
113. M.Fouletier, P.Degott, and M.B.Armand, Solid State Ionics, 1983, **8**, 165.
114. G.Leising, F.Stelzer, and H.Kahlert, J.Phys.(France): Colloq., 1984, **44**, C3–139.
115. J.B.Torrance and B.D.Silverman, Phys.Rev., 1977, **B15**, 788.
116. G.Wegner, Makromol.Chem.Macromol.Symp., 1986, **1**, 151.
117. T.P.H.Jones, G.R.Mitchell, and A.H.Windle, Colloid and Polym.Sci., 1983, **261**, 110.
118. V.A.Legasov and A.L.Buchachenko, Uspekhi Khim., 1986, **55**, 1949 [Russ.Chem.Rev., 1986(12)].

Gor'kii Khar'kov
State University